Decoding the Pattern of Photon Colors in Single-Molecule FRET

Irina V. Gopich* and Attila Szabo

Laboratory of Chemical Physics, National Institute of Diabetes and Digestive and Kidney Diseases, National Institutes of Health, Bethesda, Maryland 20892

Received: April 21, 2009; Revised Manuscript Received: June 15, 2009

Conformational dynamics of a single molecule can be studied using Förster resonance energy transfer (FRET) by recording a sequence of photons emitted by a donor and an acceptor dye attached to the molecule. We describe a simple and robust method to estimate the rates of transitions between different conformational states and the FRET efficiencies associated with these states. For a photon trajectory with measured interphoton times, the pattern of colors is decoded by maximizing the appropriate likelihood function. This approach can be used to analyze bursts of photons from diffusing molecules as well as photon trajectories generated by immobilized molecules. The procedure is illustrated using simulated photon trajectories corresponding to two-state and three-state molecules. The method works even when the photon colors appear to be scrambled because of high background noise, the photophysical properties of the conformers are similar, or the conformational and photon count rates are comparable. The consistency of the model with the data can be checked by recoloring the photon trajectories and comparing the predicted and observed FRET efficiency histograms.

I. Introduction

Single-molecule Förster resonance energy transfer (FRET) is a powerful technique to study biological molecules.[1−3] The output of such measurements is a photon trajectory, that is, a sequence of photons with different colors emitted by the donor and acceptor dyes attached to a molecule. The probability that a photon is emitted by the donor or by the acceptor depends on the distance between them. Therefore, the pattern of photon colors contains information about the interdye distance that is modulated by the molecule's conformational dynamics. The molecule under study can be attached to a surface or diffuse through a laser spot. The advantage of the diffusion experiments is that the molecule cannot interact with a surface. A photon trajectory in diffusion measurements is a set of short bursts generated by different single molecules traversing the laser spot. The statistics of photon counts in a burst depends on both the location of the molecule in the laser spot and the interdye distance.

Two-colored photon trajectories are often analyzed using FRET efficiency histograms.[4] The trajectories are first divided into time bins, or alternatively, bursts of photons are selected using a search algorithm. The FRET efficiency in each bin or burst is obtained as the ratio of the number of acceptor photons to the total number of photons. This ratio fluctuates because of various stochastic processes, of which, only fluctuations of interdye distance due to conformational dynamics are usually of interest.

Although significant progress in analyzing FRET efficiency histograms has been made,[5−9] it is still challenging to extract quantitative information about conformational dynamics from them. There are several reasons for this. First, an efficiency histogram is a reduced representation of a whole photon trajectory[10] and thus might not be sufficiently sensitive to the parameters of conformational dynamics. Second, in order to quantitatively describe FRET efficiency histograms obtained from diffusing molecules, one needs additional information such as the dependence of the photon count rate on the molecule's location in the laser spot. When the interdye distance does not change during the observation time, this can be circumvented, and the FRET efficiency distribution can be reconstructed using the measured distribution of the sum of donor and acceptor photons.[5,6] However, when conformational transitions occur on a time scale comparable to the bin or the burst duration, this procedure can be generalized only approximately, assuming that the sum of donor and acceptor count rates does not fluctuate as a molecule traverses the laser spot.[11] Finally, although there is a rigorous theory for the FRET efficiency histograms,[11,12] an analytical solution is available only for two-state conformational dynamics. For models with more than two states, the calculation of the histograms is rather involved.[10]

Recently, we introduced an alternate approach in which the whole photon trajectory is analyzed by maximizing a likelihood function.[11] In this paper, we further develop this method for extracting structural and kinetic parameters from a sequence of photon colors and interphoton times. Using simulated photon trajectories, we show that the conformational parameters can be readily obtained even when the transition rates between the conformational states are as fast as the photon count rate.

Maximum likelihood-based analyses of time sequences have been performed in a variety of contexts, including ion channels,[13−15] molecular motors,[16] protein dynamics,[17] and single-molecule fluorescence spectroscopy.[18−21] Long trajectories of donor and acceptor photons emitted by immobilized molecules can be binned and converted to FRET efficiency trajectories, which can be then analyzed using hidden Markov models.[22,23] Extension of these methods to diffusing molecules with conformational dynamics is challenging because the photon count rate fluctuates when a molecule traverses the laser spot.[21] In addition, a short photon trajectory generated by a diffusing molecule cannot be accurately converted into a FRET efficiency trajectory. Our method does not require binning of photons and does not involve photon count rates. It is based only on the

* To whom correspondence should be addressed.

10.1021/jp903671p
Published on Web 07/09/2009

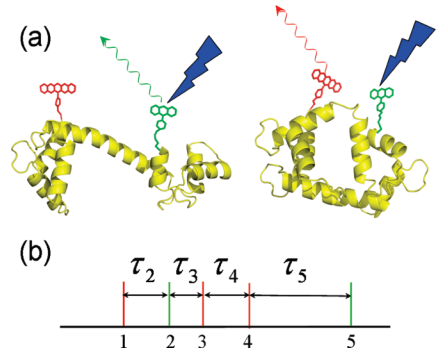

Figure 1. (a) Cartoon of a protein with attached donor (green) and acceptor (red) dyes that can exist in two conformations. After excitation by blue light, the donor can emit a green photon, or the excitation energy can be transferred to the acceptor, which then can emit a red photon. (b) An example of a trajectory of acceptor (red) and donor (green) photons. Note that for notational convenience, we have defined τ_k as the time between the kth and $(k-1)$th photon; therefore, the first interphoton time is τ_2.

probability of photon colors. In this way, we avoid the analysis and modeling of translational diffusion. Although the method is valid for both immobilized and diffusing molecules, our primary focus here is on its application to diffusion measurements.

The outline of the paper is as follows. In the next section, we present the procedure of decoding the pattern of photon colors. Section III gives illustrative examples which deal with extracting the parameters of a two-state model, treating the influence of background noise, and comparing different models based on recoloring and on likelihoods. The theoretical basis of the method is presented in section IV. Concluding remarks are given in the last section.

II. The Decoding Procedure

In this section, we describe our method and present the formulas required to implement it. The theoretical foundation will be given in section IV.

A sequence of photons (a photon trajectory) emitted by a molecule diffusing through a laser spot is characterized by interphoton times and by photon colors (see Figure 1). Photon statistics are affected by various stochastic processes. These can be classified as fast or slow compared to the average time between detected photons, which is usually on the μs time scale. Fast processes include photophysical processes (e.g., excitation, decay, energy transfer) as well as dye reorientation and interdye distance fluctuations (from linker motion or conformational dynamics) that occur on the submicrosecond time scale. Slow processes include translational diffusion through the laser spot and conformational dynamics that occur on the time scale comparable to, or slower than, the interphoton time.

In the absence of slow processes, the photons are assumed to be uncorrelated and to obey Poisson statistics. The Poisson distribution is completely characterized by the acceptor and donor count rates, n_A and n_D, which are the mean number of acceptor and donor photons per unit time. In general, count rates are determined by the steady-state populations of the donor and acceptor excited states that are calculated assuming that the slow dynamics are frozen.[12] In the simplest example of a donor−acceptor pair with fixed interdye distance and low laser excitation, $n_A = \phi_A\eta_A k_{ex}k_{tr}/(k_D + k_{tr})$ and $n_D = \phi_D\eta_D k_{ex}k_D/(k_D + k_{tr})$, where $\phi_{A,D}$ and $\eta_{A,D}$ are the quantum yields and detection efficiencies of acceptor and donor photons, k_{ex} and k_D are the donor excitation and decay rates, and k_{tr} is the rate of energy transfer, which depends on the interdye distance r as $k_{tr} = k_D(R_0/r)^6$, where R_0 is the Förster radius. The apparent energy transfer efficiency is defined here as the ratio of the acceptor count rate to the total count rate, $\epsilon = n_A/(n_A + n_D)$. For this example, it is $\epsilon = \gamma/(\gamma + (r/R_0)^6)$, where $\gamma = \phi_A\eta_A/\phi_D\eta_D$ is the gamma factor.[36] If there is cross talk (i.e., leakage of donor photons into the acceptor channel), then the above expression for n_A must be modified by adding a term cn_D.[24] The apparent efficiency now becomes $\epsilon = (\gamma + c(r/R_0)^6)/(\gamma + (1+c)(r/R_0)^6)$. Note that both cross talk and unequal detection efficiencies ($\gamma \neq 1$) do not alter the definition of the apparent transfer efficiency but rather modify its functional dependence on the interdye distance. In fact, this is the case for all photophysical and conformational processes that are faster than the count rates and for other complications such as direct excitation of the acceptor.

The count rates depend on the conformational state (through the energy transfer rate) and on the location in the laser spot (through the excitation rate and the detection efficiencies). When both conformation and location in the laser spot are fixed, the statistics of photons are Poissonian. When the conformational state and/or the location in the laser spot changes, the count rates fluctuate, and the photon statistics are no longer Poissonian.

The distribution of the times between photons regardless of their color is determined by the sum of the donor and acceptor count rates. If the total count rate is independent of the conformation, then the times between photons depend only on the location in the spot. These times contain information about diffusion through the laser spot but not about conformational dynamics.

Now consider the photon colors. The probability that a particular photon has a certain color depends on the ratio of the acceptor and donor count rates of the conformation that emits this photon. When this ratio does not depend on the location in the laser spot, the colors of photons depend solely on the conformation. Thus, all information about conformations is contained in the pattern of photon colors. This is the key idea of the method. We can extract parameters of a proposed model of conformational dynamics by maximizing the likelihood function obtained from the probability of the observed photon colors.

Now, we give the recipe for the likelihood function. It will be justified in the Theory section. Suppose we are given a photon trajectory from an immobilized molecule or a burst of photons from a diffusing molecule with specified colors and interphoton times. We assume that the molecule emitting these photons has several conformational states. Each state is characterized by the apparent FRET efficiency ϵ_i, which is defined as the ratio of the acceptor count rate to the total count rate. Some states may have the same efficiencies. The efficiencies are related to the interdye distances. The precise form of this relationship depends on the dye's photophysics, fast orientational dynamics, and the detection efficiency. The transitions between the states are described by the rate matrix $\boldsymbol{K}$. Its element K_{ij} is the rate of the $j \to i$ transition, and $K_{ii} = -\sum_{j\neq i} K_{ji}$. The likelihood function of the burst of five photons shown in Figure 1B is

$$L = \mathbf{1}^T(\boldsymbol{I} - \boldsymbol{E})e^{\boldsymbol{K}\tau_5}\boldsymbol{E}e^{\boldsymbol{K}\tau_4}\boldsymbol{E}e^{\boldsymbol{K}\tau_3}(\boldsymbol{I} - \boldsymbol{E})e^{\boldsymbol{K}\tau_2}\boldsymbol{E}\boldsymbol{p}_{eq} \qquad (1)$$

where $\boldsymbol{E}$ is the diagonal matrix with FRET efficiencies ϵ_i on the diagonal, $\boldsymbol{I}$ is the unity matrix, $\mathbf{1}^T$ is the unit row vector (T means transpose), and $\boldsymbol{p}_{eq}$ is the vector of equilibrium probabilities of conformational states (which are obtained by solving $\boldsymbol{K}\boldsymbol{p}_{eq} = 0$ with the normalization $\mathbf{1}^T\boldsymbol{p}_{eq} = 1$). The above expression should be read from the right to the left. The first

term on the right, $\boldsymbol{p}_{eq}$, arises because, initially, the system is in equilibrium. The next term $\boldsymbol{E}$ corresponds to the first detected photon, which is, in this case, red (acceptor). The evolution of the conformational states until the next photon is detected at time τ_2 is described by the matrix exponential (propagator), $\exp(\boldsymbol{K}\tau_2)$. The next term $\boldsymbol{I} - \boldsymbol{E}$ corresponds to the green (donor) photon, and so on. The final multiplication by $\mathbf{1}^T$ sums over all conformational states.

The above expression, generalized to an arbitrary number of photons (N_{ph}) in a burst, can be written as

$$L = \mathbf{1}^T \prod_{k=2}^{N_{ph}} (\boldsymbol{F}(c_k)\mathrm{e}^{\boldsymbol{K}\tau_k})\boldsymbol{F}(c_1)\boldsymbol{p}_{eq} \quad (2)$$

where $\boldsymbol{F}(c_k)$ is a matrix which depends on the color of the kth photon c_k, $\boldsymbol{F}(\text{red}) = \boldsymbol{E}$ and $\boldsymbol{F}(\text{green}) = \boldsymbol{I} - \boldsymbol{E}$, and τ_k is the time between the $(k-1)$th and kth photon. The product is taken over all photons in the burst. Equation 2 reduces the calculation of L to successive matrix−vector multiplication.

When there are several bursts of photons (or several different photon trajectories in the case of immobilized molecules), the likelihoods are multiplied. The bursts can have various durations and numbers of photons. The resulting likelihood function depends on the conformational parameters, that is, the elements of the efficiency and the rate matrices, $\boldsymbol{E}$ and $\boldsymbol{K}$. The matrix elements can be found by maximizing the log likelihood.

When conformational dynamics are slow compared to interphoton times, the matrix exponentials in eq 2 can be approximated as $\mathrm{e}^{\boldsymbol{K}\tau} \approx \boldsymbol{I} + \boldsymbol{K}\tau$. In general, to speed up the computation, the rate matrix can be diagonalized, $\boldsymbol{KU} = \boldsymbol{U}\boldsymbol{\Lambda}$, where $\boldsymbol{\Lambda}$ is the matrix with the eigenvalues λ_i on the diagonal. The likelihood function can then be written as

$$L = \boldsymbol{p}_0^T \prod_{k=2}^{N_{ph}} (\Phi(c_k)\mathrm{e}^{\Lambda\tau_k})\boldsymbol{\Phi}(c_1)\boldsymbol{p}_0 \quad (3)$$

where $\boldsymbol{\Phi}(\text{red}) = \boldsymbol{U}^{-1}\boldsymbol{E}\boldsymbol{U}$ and $\boldsymbol{\Phi}(\text{green}) = \boldsymbol{I} - \boldsymbol{U}^{-1}\boldsymbol{E}\boldsymbol{U}$, the elements of the diagonal matrix $\exp(\boldsymbol{\Lambda}\tau)$ are $\exp(\lambda_i\tau)$, and $\boldsymbol{p}_0$ is a vector with one nonzero element (equal to 1). The index of this nonzero element corresponds to the index of the zero eigenvalue of $\boldsymbol{\Lambda}$. The vector $\boldsymbol{p}_0$ is proportional to $\boldsymbol{U}^{-1}\boldsymbol{p}_{eq}$ and $\boldsymbol{p}_0^T$ to $\mathbf{1}^T\boldsymbol{U}$. All of these quantities are calculated only once for a given set of parameters.

When conformational dynamics are on a time scale much longer than the burst duration (static limit), the likelihood function of a burst simplifies to[11,25]

$$L = \sum_i \epsilon_i^{N_A}(1 - \epsilon_i)^{N_D} p_{eq}(i) \quad (4)$$

where N_A (N_D) is the number of acceptor (donor) photons in a burst. The summation is performed over all conformational states i. This likelihood function can be used only to analyze many photon trajectories, each generated by a different single molecule. The likelihood function for many bursts is a product of the likelihood functions in eq 4.

In the presence of background noise, the procedure is operationally the same. The efficiencies and the rates are found by maximizing the same likelihood function as above. The resulting efficiencies, ϵ_i^{fit}, are then transformed into corrected efficiencies ϵ_i^{cor} by using

$$\epsilon_i^{cor} = \frac{\langle n\rangle\epsilon_i^{fit} - b_A}{\langle n\rangle - b_A - b_D} \quad (5)$$

where b_A and b_D are the acceptor and donor background count rates and $\langle n\rangle$ is the total (acceptor, donor, and background) count rate averaged over the laser spot.

The above procedure is completely rigorous when the sum of the donor and acceptor count rates is independent of the conformational state and the ratio of the donor and acceptor count rates is independent of the location in the laser spot. The second condition is usually met when the ratio of the donor and acceptor detection efficiencies η_D/η_A does not depend on the location in the laser spot. The first condition is more restrictive. For the donor−acceptor pair considered at the beginning of this section, this condition is met when the gamma factor, which is the ratio of the quantum yields and detection efficiencies of the acceptor and donor photons, is equal to one in all conformational states. In the case of diffusing molecules, the method is valid for sufficiently low concentrations of the molecules, so that only one molecule is in the laser spot at a given time.[26] It is assumed here that the translational diffusion coefficient does not depend on the conformations.

The likelihood function in eq 2 is obtained from the probability of observing photon colors in a trajectory with given interphoton times. When the above requirements are not satisfied, the likelihood function can be generalized by considering the probability of observing both colors and interphoton times. For a diffusing molecule, it is rather complex (see section IV). However for a single immobilized molecule, the likelihood function is quite simple. Instead of FRET efficiencies ϵ_i, it now involves the donor, n_{Di}, and acceptor, n_{Ai}, count rates, and can be written as:

$$L = \mathbf{1}^T \prod_{k=2}^{N_{ph}} (\boldsymbol{F}(c_k)\mathrm{e}^{(\boldsymbol{K}-\boldsymbol{N})\tau_k})\boldsymbol{F}(c_1)\boldsymbol{p}_{eq}/\mathbf{1}^T\boldsymbol{N}\boldsymbol{p}_{eq} \quad (6)$$

where $\boldsymbol{F}(\text{red}) = \boldsymbol{N}_A$ and $\boldsymbol{F}(\text{green}) = \boldsymbol{N}_D$. Here, $\boldsymbol{N}_A$ and $\boldsymbol{N}_D$ are diagonal matrices with the acceptor, n_{Ai}, and donor, n_{Di}, count rates on the diagonal, and $\boldsymbol{N} = \boldsymbol{N}_A + \boldsymbol{N}_D$ has diagonal elements $n_i = n_{Ai} + n_{Di}$. This likelihood function can also be used to analyze colorless photon trajectories[21] by setting $\boldsymbol{F} = \boldsymbol{N}$. In the presence of background noise, one can still use eq 6 to extract n_{Ai}^{fit} and n_{Di}^{fit} and the rates. The corrected count rates are obtained by shifting the extracted count rates $n_{Ai}^{cor} = n_{Ai}^{fit} - b_A$ and $n_{Di}^{cor} = n_{Di}^{fit} - b_D$. When the total count rate does not depend on states ($\boldsymbol{N} = n\boldsymbol{I}$, where n is a number), then $\boldsymbol{N}_A = n\boldsymbol{E}$ and $\boldsymbol{N}_D = n(\boldsymbol{I} - \boldsymbol{E})$, and thus, eq 6 reduces to eq 2 within a factor that does not depend on the conformational parameters. The likelihood function in eq 6 is exact when the photon statistics in each conformational state is Poissonian.

The matrix exponential in the above expression can be calculated via matrix diagonalization, as mentioned earlier. When conformational dynamics are slow compared to the photon count rates, it can be shown that the matrix exponential simplifies to

$$[\mathrm{e}^{(\boldsymbol{K}-\boldsymbol{N})\tau}]_{ij} \approx \mathrm{e}^{-n_i\tau}\delta_{ij} + K_{ij}\frac{\mathrm{e}^{-n_i\tau} - \mathrm{e}^{-n_j\tau}}{n_i - n_j} \quad (7)$$

where δ_{ij} is the Kronecker delta, which is 1 if $i = j$ and 0 otherwise. The term multiplying K_{ij} has a simple physical

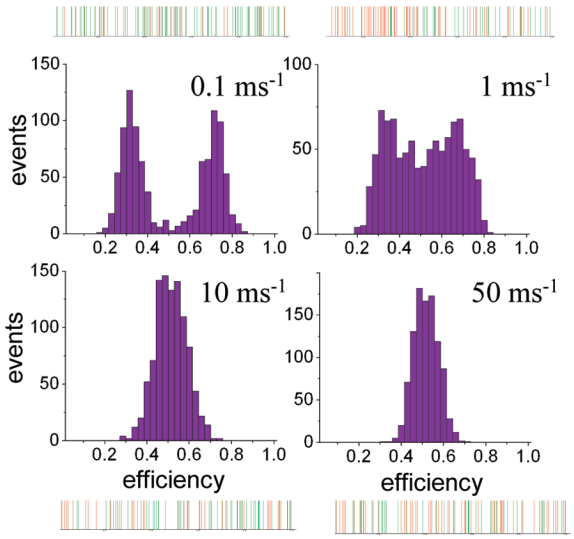

Figure 2. FRET efficiency histograms obtained from 1000 1 ms bursts of photons emitted by a molecule with two conformational states. Examples of bursts are above or below the corresponding histograms. In all panels, the photon count rates used to generate the bursts are $n_{A1} = n_{D2} = 30\ \mathrm{ms}^{-1}$ and $n_{A2} = n_{D1} = 70\ \mathrm{ms}^{-1}$, so that the efficiencies in the two states are $\epsilon_1 = 0.3$ and $\epsilon_2 = 0.7$. The transition rates $k_1 = k_2$ are shown in the upper right corner of each histogram.

interpretation. It is proportional to the distribution of the times between two consecutive photons when a single conformational transition occurs during the time between them.

III. Illustrative Applications

A. Two-State Dynamics. Let us use the above procedure to analyze photon trajectories emitted by a molecule with two conformational states. When the molecule is in state i ($i = 1$, 2), the photon statistics are Poissonian with the count rates n_{Ai} and n_{Di} for the acceptor and donor photons. The transition rates are $K_{21} = k_1$ ($1 \rightarrow 2$) and $K_{12} = k_2$ ($2 \rightarrow 1$). We generate bursts of photons by simulating this kinetic scheme and then apply the procedure described above to extract the conformational parameters, that is, the FRET efficiencies, ϵ_1 and ϵ_2 ($\epsilon_i = n_{Ai}/(n_{Ai} + n_{Di})$), and the rates k_1 and k_2.

The bursts of photons are generated using an algorithm similar to Gillespie's,[27] in which the times between successive events are generated from the appropriate distribution. There are three types of events, namely, detection of an acceptor or a donor photon or a conformational transition. The times between these events are drawn from the exponential distribution, $(n_{Ai} + n_{Di} + k_i)\exp(-(n_{Ai} + n_{Di} + k_i)\tau)$ when the molecule is in state $i = 1$, 2. The type of the event (i.e., a conformational transition or the detection of an acceptor or a donor photon) is chosen according to the probabilities $\{k_i/(n_{Ai} + n_{Di} + k_i), n_{Ai}/(n_{Ai} + n_{Di} + k_i), n_{Di}/(n_{Ai} + n_{Di} + k_i)\}$. The initial state is chosen according to the equilibrium distribution, $\{k_2/(k_1 + k_2), k_1/(k_1 + k_2)\}$.

FRET efficiency histograms obtained from 1000 simulated bursts, each containing 100 photons on average, are shown in Figure 2, along with examples of the bursts. Conformational dynamics vary from very slow (1 transition per 10 bursts) to very fast (the time between transitions is comparable to the interphoton time). To extract the conformational parameters, the likelihood function is calculated using eq 2. For the two-state molecule

$$\boldsymbol{E} = \begin{pmatrix} \epsilon_1 & 0 \\ 0 & \epsilon_2 \end{pmatrix} \qquad \boldsymbol{K} = \begin{pmatrix} -k_1 & k_2 \\ k_1 & -k_2 \end{pmatrix} \qquad \boldsymbol{p}_{eq} = \begin{pmatrix} p_1 \\ p_2 \end{pmatrix} \tag{8}$$

where $p_1 = 1 - p_2 = k_2/(k_1 + k_2)$. The eigenvalues of $\boldsymbol{K}$ are 0 and $-(k_1 + k_2)$, and the transformed matrices (see eq 3) are

$$\boldsymbol{U}^{-1}\boldsymbol{E}\boldsymbol{U} = \begin{pmatrix} \epsilon_1 p_1 + \epsilon_2 p_2 & (\epsilon_2 - \epsilon_1)p_2 \\ (\epsilon_2 - \epsilon_1)p_1 & \epsilon_1 p_2 + \epsilon_2 p_1 \end{pmatrix}$$
$$\exp(\boldsymbol{\Lambda}\tau) = \begin{pmatrix} 1 & 0 \\ 0 & e^{-(k_1+k_2)\tau} \end{pmatrix} \qquad \boldsymbol{p}_0 = \begin{pmatrix} 1 \\ 0 \end{pmatrix} \tag{9}$$

The parameters of the model were extracted by maximizing the sum of the log likelihood functions for each burst, eq 3, using Mathematica (Wolfram Research, Inc.) built-in functions. Standard deviations were obtained from the curvature of the log likelihood function at the maximum (i.e., the square roots of the diagonal elements of the inverse Hessian matrix). All four parameters of the model were determined by this maximization procedure.

The extracted parameters are shown in Table 1. It would be difficult to obtain this information from the efficiency histograms in Figure 2 in all cases. For example, only the peak position (mean FRET efficiency) and the width (mainly due to shot noise) can be obtained from the last histogram. However, our method allows one to obtain the model parameters both in the case of fast (i.e., comparable to the time between photons) and slow (slower than the burst duration) transition rates. The uncertainty in the parameters increases when the dynamics become very fast. When dynamics are slow, the efficiencies are determined very accurately, but the uncertainty in rates increases. When the transition rates are in the optimal range (1 and 10 ms^{-1}), standard deviations are around 1% for the efficiencies and 5% for the rates. It should be noted that in this example, the only source of error in the extracted parameters is the lack of data (i.e., only 1000 bursts were used). The accuracy increases when the total number of photons increases.

B. Background Noise. We now show that the above procedure gives reliable rates and efficiencies even in the presence of background noise. Poissonian background photon counts were added to the photon trajectories generated with the same parameters as those in the previous example and $k_1 = k_2 = 1\ \mathrm{ms}^{-1}$. High background noise can substantially transform the shape of the FRET efficiency histogram (see Figure 3). We applied the same procedure as before to the trajectories with background noise. It is remarkable that although the extracted efficiencies $\epsilon_{1,2}^{fit}$ are shifted compared to the exact ones, the rates are still correct, even when there are as many background photons as photons emitted by the molecule (see Table 2). When the fitted efficiencies were corrected using eq 5, they were in a good agreement with the "true" efficiencies ($\epsilon_1 = 0.3$ and $\epsilon_2 =$

TABLE 1: Parameters Extracted from the Photon Bursts in Figure 2[a]

k_1, k_2 (ms^{-1})	k_1 (ms^{-1})	k_2 (ms^{-1})	ϵ_1	ϵ_2
0.1	0.115 (0.014)	0.113 (0.014)	0.301 (0.002)	0.702 (0.002)
1	0.994 (0.054)	0.985 (0.054)	0.303 (0.002)	0.701 (0.002)
10	9.44 (0.42)	10.0 (0.44)	0.308 (0.0045)	0.707 (0.0047)
50	56.8 (4.5)	48.7 (4.1)	0.278 (0.013)	0.689 (0.011)

[a] Standard deviations are given in parentheses. Photon bursts were generated using $\epsilon_1 = 0.3$ and $\epsilon_2 = 0.7$, and the transition rates $k_1 = k_2$ are shown in the left column.

TABLE 2: Extracted Conformational Parameters from Photon Trajectories with Background Noise[a]

b_A (ms^{-1})	b_D (ms^{-1})	k_1 (ms^{-1})	k_2 (ms^{-1})	ϵ_1^{fit}	ϵ_2^{fit}	ϵ_1^{cor}	ϵ_2^{cor}
20	30	1.05 (0.065)	1.03 (0.064)	0.333 (0.002)	0.598 (0.002)	0.299	0.697
50	50	0.99 (0.066)	0.92 (0.063)	0.398 (0.002)	0.602 (0.002)	0.296	0.704

[a] Standard deviations are given in parentheses. Parameters used to generate "true" photon trajectories are the same as those in Figure 2, with $k_1 = k_2 = 1$ ms^{-1}. Background count rates b_A and b_D are given in the left column. Transition rates k_1 and k_2 and efficiencies ϵ_1^{fit} and ϵ_2^{fit} are obtained by applying the procedure in section II. The efficiencies are then corrected using eq 5.

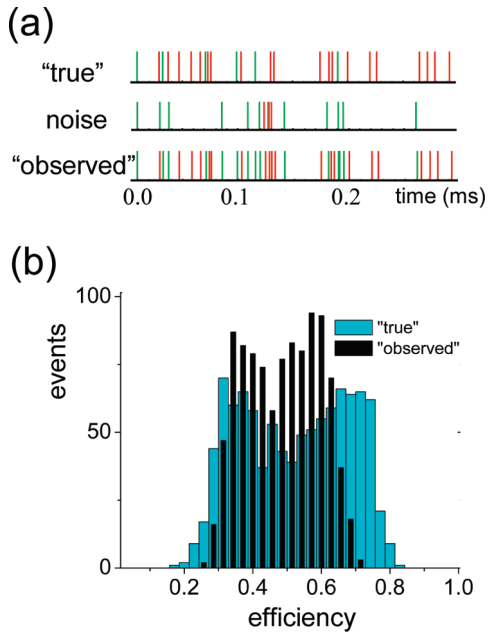

Figure 3. (a) Example of a photon trajectory with added background photons ("true" + noise = "observed"). (b) FRET efficiency histograms obtained from 1000 1 ms bursts with true photons (cyan) and with added background noise (black). Parameters used to generate the photon trajectories are $k_1 = k_2 = 1$ ms^{-1}, $\epsilon_1 = 0.3$, and $\epsilon_2 = 0.7$. The sum of the donor and acceptor count rates is 100 ms^{-1} in both states, and the background count rates are $b_A = 20$ ms^{-1} (acceptor) and $b_D = 30$ ms^{-1} (donor).

0.7) used to generate bursts. This correction procedure is exact for the simulated bursts of photons, so that we get very accurate rates and corrected efficiencies despite the big difference in the histograms in the presence and absence of noise.

C. Recoloring. How can we check that the model used can adequately describe the data? In particular, one would like to see how the observed FRET efficiency histograms agree with those predicted by the model. Since we do not extract all of the parameters that define the photon trajectory, we cannot generate a new set of photon trajectories and construct a FRET efficiency histogram from them. However, we can recolor the experimental photon trajectories using only the conformational parameters. In this method, we first wipe out the colors of the observed photon trajectory without changing the times between photons. Then, the trajectory is recolored in accordance with the likelihood function in eq 2.

The algorithm for recoloring is as follows. The initial state is drawn from the equilibrium probability. If this state is i, the color of the first photon is chosen to be the acceptor or donor with probabilities (ϵ_i, $1 - \epsilon_i$). The state j at the moment the second photon is detected is chosen with probability $[\exp(\boldsymbol{K}\tau)]_{ji}$, where τ is the time between the first and the second photons. This procedure is then repeated. In this way, we get a new photon trajectory with the same times between photons as the measured one but with different colors. The recolored trajectory is then used to obtain a new FRET efficiency histogram, which is then compared with the observed one.

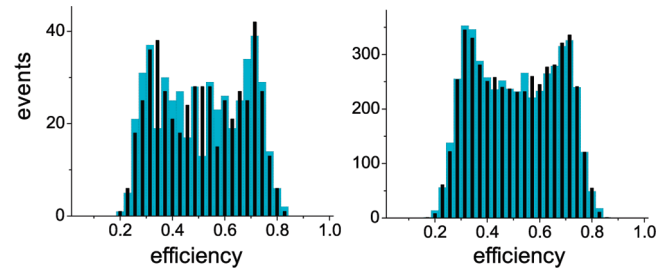

Figure 4. Comparison of the FRET efficiency histogram obtained from the "observed" (cyan) and "recolored" (black) bursts of photons (500 and 5000 bursts on the left and right panels, respectively). The parameters are the same as those in Figure 2, with $k_1 = k_2 = 1$ ms^{-1}.

Figure 4 shows examples of the efficiency histograms obtained from recolored trajectories. The cyan histograms are obtained from the "observed" bursts of photons, and the black ones are obtained from the recolored bursts. The deviation between the histograms in the left panel is due to lack of statistics. When the number of bursts is increased from 500 (left) to 5000 (right), the deviation between the "observed" and "recolored" histograms becomes very small. By recoloring the same trajectory several times with the same model parameters, one can determine whether the deviation between the histograms is due to a bad model or insufficient data.

To illustrate how recoloring can help to select the right model, consider a three-state system

$$\epsilon_1 \underset{k_2}{\overset{k_1}{\rightleftharpoons}} \epsilon_2 \underset{k_4}{\overset{k_3}{\rightleftharpoons}} \epsilon_3 \qquad (10)$$

The photon bursts corresponding to this scheme are generated by adapting the algorithm described previously. The simulated data are then analyzed to extract FRET efficiencies and rates using the likelihoods corresponding to the two-state and the three-state models. The generated bursts are then recolored using these extracted parameters.

In the first example, the equilibrium populations of the three states with the efficiencies 0.3, 0.5, and 0.8 are in the ratio 1:2:4. Figure 5 shows the histograms obtained from the simulated bursts of photons (left) and from the recolored bursts (right) using the parameters of the two-state model that are obtained by maximizing the likelihood. For these parameters, the histograms clearly show that the two-state model is not consistent with the data. As expected, recoloring the trajectory with the parameters of the three-state model results in the correct histogram (not shown). Thus, in this case, the three-state model can be selected by comparing the "observed" and "recolored" histograms.

However, FRET efficiency histograms, being a reduced representation of the data, do not always show the difference between the models so clearly. Consider the histograms shown in Figure 6. Here, there are three states with efficiencies 0.3, 0.5, and 0.7, which are equally populated. As in the previous

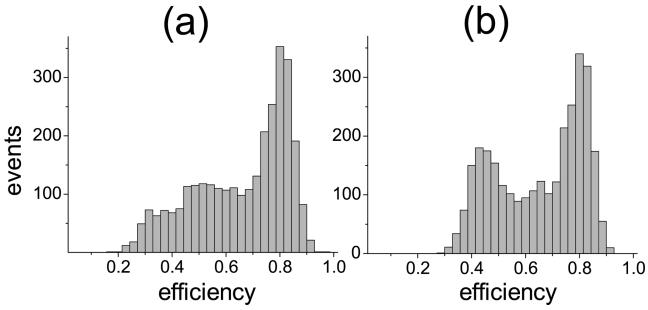

Figure 5. Comparison of models using recoloring. (a) The histogram obtained from the "observed" bursts of photons emitted by a molecule with three conformational states. Parameters used to generate the trajectories are (see eq 10) $k_1 = k_3 = 1$ ms^{-1}, $k_2 = k_4 = 0.5$ ms^{-1}, $\epsilon_1 = 0.3$, $\epsilon_2 = 0.5$, and $\epsilon_3 = 0.8$. There are 3000 bursts of 1 ms duration with the count rate $n_{Ai} + n_{Di} = 100$ ms^{-1} in each state. (b) The histogram from bursts recolored using the two-state model with parameters $\epsilon_1 = 0.41$, $\epsilon_2 = 0.79$, $k_1 = 0.74$, and $k_2 = 0.48$ that were obtained by maximizing the log likelihood.

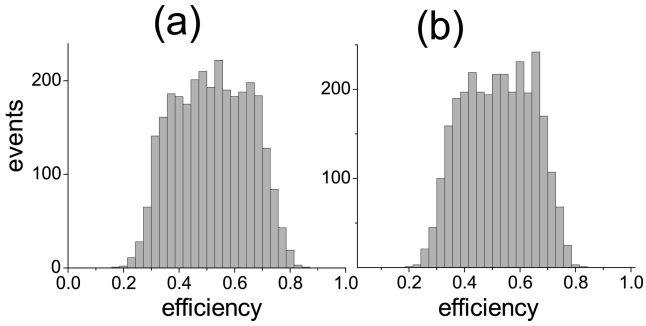

Figure 6. Recoloring as in Figure 5 but with different parameter values. (a) The histogram obtained from the 3000 "observed" bursts of photons emitted by a molecule with three conformational states, $k_1 = k_2 = k_3 = k_4 = 2$ ms^{-1}, $\epsilon_1 = 0.3$, $\epsilon_2 = 0.5$, and $\epsilon_3 = 0.7$. (b) The histogram from bursts recolored using the two-state model with parameters $\epsilon_1 = 0.34$, $\epsilon_2 = 0.66$, $k_1 = 1.24$, and $k_2 = 1.17$ that were obtained by maximizing the log likelihood.

example, the "observed" histogram (left) is compared with the "recolored" one (right), which is based on the two-state model. The histograms look similar, and it may appear that the two-state model is sufficient to describe the data. To show that the three-state model is actually preferable in this case, we can use the Bayesian information criterion[28] (BIC), defined as

$$\mathrm{BIC} = -2 \ln L_m + M_p \ln N_d \tag{11}$$

where L_m is the maximum value of the likelihood function, M_p is the number of free parameters to be estimated, and N_d is the number of data points (photons in this case). The model with the lower value of BIC is the better one. For data of good quality, the dominant contribution to BIC comes from the first term. For the example in Figure 6, the log likelihood of the three-state model is greater than that of the two-state model by 250. The second term penalizes for additional fitting parameters (three extra parameters for the three-state system) but does not come close to beating the difference in log likelihoods. Therefore, the three-state model is preferable in this case, as it should be. More details about model selection can be found in refs 29−31.

D. Total Count Rate Depends on Conformational State. Now, let us consider the case when the total count rate depends on the conformational state. This occurs, for instance, when the gamma factor (which is the ratio of the quantum yields and detection efficiencies of the acceptor and donor photons) is not equal to 1. When only the rate of energy transfer depends on conformation, the gamma factor can be made equal to 1 by randomly discarding photons following the procedure of ref 6. However, this does not help when there is another state-dependent process that influences photon count rates, such as differential quenching of the states.[32] If the total count rate depends on the conformational state, both the photon colors and the interphoton times depend on conformational parameters. As a consequence, the likelihood of photon colors in eq 2 is not rigorously correct.

TABLE 3: Examples of Conformational Parameters Extracted from Only the Photon Colors When the Total Donor and Acceptor Count Rate Depends on the Conformation[a]

k_1,k_2 (ms^{-1})	k_1 (ms^{-1})	k_2 (ms^{-1})	ϵ_1	ϵ_2
0.1	0.12 (0.014)	0.11 (0.013)	0.304 (0.002)	0.701 (0.0014)
1.0	1.09 (0.06)	0.95 (0.05)	0.297 (0.002)	0.697 (0.002)
10.0	12.32 (0.44)	7.03 (0.26)	0.275 (0.0046)	0.686 (0.002)
50.0	74.1 (4.3)	26.8 (2.1)	0.251 (0.01)	0.668 (0.005)

[a] The parameters (and standard deviations in parentheses) are obtained from 1000 1 ms bursts. The bursts were generated using $n_{A1} = 30$ ms^{-1}, $n_{D1} = 70$ ms^{-1}, $n_{A2} = 140$ ms^{-1}, $n_{D2} = 60$ ms^{-1} (so that $\epsilon_1 = 0.3$ and $\epsilon_2 = 0.7$), and transition rates ($k_1 = k_2$) that are shown in the left column.

Nevertheless, consider what happens when we use this formula to analyze data generated when the total count rates are conformation-dependent. Consider a two-state system with the parameters given in Figure 2, except that the total count rates of the two conformations differ by a factor two. Specifically, the total count rates are $n_{A1} + n_{D1} = 100$ ms^{-1} and $n_{A2} + n_{D2} = 200$ ms^{-1} in the two states. The apparent FRET efficiencies are $\epsilon_1 = n_{A1}/(n_{A1} + n_{D1}) = 0.3$ and $\epsilon_2 = n_{A2}/(n_{A2} + n_{D2}) = 0.7$.

The examples of the parameters extracted by maximizing the likelihood in eq 2 are shown in Table 3. It is interesting that although the likelihood function is not rigorous in this case, it works surprisingly well for slow dynamics (transition rates of 0.1 and 1 per ms). However, it breaks down when the dynamics are comparable to the photon count rate. Of course, if we analyze this data by using the likelihood function in eq 6, we extract essentially exact parameters.

Thus, maximizing the likelihood function in eq 2 may result in reasonable conformational parameters, even when the total count rate depends on conformational states. This occurs when interconversion rates are slow and the FRET efficiencies of the states are well separated. In this case, the main contribution to the likelihood function comes from one state trajectory, for which conformational parameters can be found by considering only the probability of photon colors.

IV. Theory

In this section, we give a detailed explanation of the formulas presented in section II. We begin by considering the simplest case of one conformational state and gradually increase the complexity by treating the effects of conformational dynamics, translational diffusion, and background noise.

Consider the simple photon trajectory consisting of two acceptor and one donor photon shown in Figure 7. If the photons are emitted by a molecule that has only one conformational state, the probability density function (pdf) of observing this trajectory is

$$f = n_D e^{-n\tau_3} n_A e^{-n\tau_2} n_A / n \quad (12)$$

where n_A (n_D) is the acceptor (donor) count rate and $n = n_A + n_D$ is the total count rate. Reading this expression from right to left, the first term, n_A/n, is the probability that the first photon was emitted by the acceptor dye. The exponential $\exp(-n\tau_2)$ is the probability that no photons were detected during the time interval τ_2, and so on.

When there are several interconverting conformational states, the acceptor and donor count rates, n_{Ai} and n_{Di}, depend on the state i. The pdf of observing this photon trajectory, since it may result from any state trajectory, is

$$f = \sum_{i,j,k} n_{Dk} G(k, \tau_3|j) n_{Aj} G(j, \tau_2|i) n_{Ai} p_{eq}(i) / \langle n \rangle \quad (13)$$

where $G(j,\tau|i)$ is the probability that the molecule is in state j at time τ given it was in state i initially and that no photons were detected during this time interval, $p_{eq}(i)$ is the equilibrium probability of state i, and $\langle n \rangle = \sum_j (n_{Aj} + n_{Dj}) p_{eq}(j)$ is the average count rate. The summation is performed over all conformational states. The above expression (read right to left) has the following interpretation. The photon trajectory starts with an acceptor photon emitted by the molecule in state i, $n_{Ai} p_{eq}(i)/\langle n \rangle$; the molecule goes to state j without photons being detected during time τ_2, $G(j,\tau_2|i)$; an acceptor photon emitted from this state is detected at time τ_2, n_{Aj}; the molecule switches from j to k without photons being detected during time τ_3, $G(k,\tau_3|j)$; and the final donor photon is detected at time τ_3, n_{Dk}.

To find $G(j,t|i)$, one must eliminate the possibility that a photon is detected during time t. This can be done by adding an irreversible sink term to the conventional rate equation that describes conformational dynamics. Then, the matrix of the transition probabilities $\boldsymbol{G}$ with the elements $G(j,t|i)$ satisfies[33]

$$\frac{d}{dt}\boldsymbol{G} = \boldsymbol{K}\boldsymbol{G} - \boldsymbol{N}\boldsymbol{G} \quad (14)$$

where $\boldsymbol{K}$ is the rate matrix describing conformational dynamics and $\boldsymbol{N}$ is a diagonal matrix with the total count rates $n_i = n_{Ai} + n_{Di}$ on the diagonal. The solution of this equation is a matrix exponential, $\boldsymbol{G}(\tau) = \exp((\boldsymbol{K} - \boldsymbol{N})\tau)$, which appears in eq 6.

Introducing the diagonal matrices $\boldsymbol{N}_A$ and $\boldsymbol{N}_D$ with the elements n_{Ai} and n_{Di} on the diagonal, the pdf in eq 13 can be rewritten in matrix notation as follows

$$f = \mathbf{1}^T \boldsymbol{N}_D e^{(\boldsymbol{K}-\boldsymbol{N})\tau_3} \boldsymbol{N}_A e^{(\boldsymbol{K}-\boldsymbol{N})\tau_2} \boldsymbol{N}_A \boldsymbol{p}_{eq} / \langle n \rangle \quad (15)$$

where $\langle n \rangle = \mathbf{1}^T \boldsymbol{N} \boldsymbol{p}_{eq}$, $\boldsymbol{I}$ is the identity matrix, and $\boldsymbol{p}_{eq}$ is the vector of equilibrium probabilities. An analogous expression was obtained for colorless trajectories by Kou et al.[21] Generalizing the above expression to an arbitrary number of photons in a burst and considering it as a function of the model parameters, we get the likelihood function in eq 6. In this function, the total count rates may depend on conformational states.

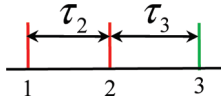

Figure 7. A photon trajectory consisting of two acceptor photons followed by a donor photon.

The above pdf and the likelihood function in eq 6 are based on the assumption that the statistics of detected photons that were emitted by the molecule in a given conformational state is Poissonian. This is true when the times between photons are much longer than the lifetime of the excited state that emits these photons. This is an excellent approximation when the detection efficiency is low and therefore the times between detected photons are much longer than the photophysical relaxation time. When this is not the case, the likelihood can be generalized. The resulting expression has the same structure as eqs 15 and 6 (see eq 43 in ref 34). However, the rate matrix $\boldsymbol{K}$ now corresponds to a more general kinetic scheme that includes both photophysical and conformational states. In addition, the diagonal matrices $\boldsymbol{N}_A$, $\boldsymbol{N}_D$, and $\boldsymbol{N} = \boldsymbol{N}_A + \boldsymbol{N}_D$ are replaced by the off-diagonal ones, $\boldsymbol{V}_A$, $\boldsymbol{V}_D$, and $\boldsymbol{V} = \boldsymbol{V}_A + \boldsymbol{V}_D$. The only nonzero elements of these matrices are the rates of transitions between excited and ground electronic states that result in acceptor or donor photons.[33,34] In this more general formalism, the likelihood function for a two-color photon trajectory has the same mathematical structure as the one for a non-Markovian two-state trajectory.[35]

When the total count rate does not depend on the conformational state, then $\boldsymbol{N} = n\boldsymbol{I}$ ($n \equiv n_{Ai} + n_{Di}$ independent of i), $\boldsymbol{N}_A = n\boldsymbol{E}$, and $\boldsymbol{N}_D = n(\boldsymbol{I} - \boldsymbol{E})$. In this case, $\exp((\boldsymbol{K} - \boldsymbol{N})\tau) = \exp(\boldsymbol{K}\tau)\exp(-n\tau)$, so that eq 15 becomes

$$f = n^2 e^{-n(\tau_2+\tau_3)} \mathbf{1}^T (\boldsymbol{I} - \boldsymbol{E}) e^{\boldsymbol{K}\tau_3} \boldsymbol{E} e^{\boldsymbol{K}\tau_2} \boldsymbol{E} \boldsymbol{p}_{eq} \quad (16)$$

The first factor $n^2 \exp(-n(\tau_2 + \tau_3))$ is the pdf of the photon trajectory when the colors are ignored, and the second is the probability of observing the color pattern, given the interphoton times. The first factor does not depend on the conformational parameters. Therefore, it can be ignored, and only the second factor must be optimized with respect to the conformational parameters. Generalizing this to an arbitrary number of photons, we arrive at eq 2 for the likelihood function. An analogous factorization will be used below to separate translational diffusion and conformational dynamics.

Let us now consider both conformational dynamics and translational diffusion. When a molecule diffuses through the laser spot, the count rates $n_{Ai}(R)$ and $n_{Di}(R)$ depend not only on the conformational state i but also on the translational coordinate R, which is the vector specifying the location of the molecule in the laser spot. The pdf of the photon trajectory in Figure 7 now becomes

$$f = \int \mathbf{1}^T \boldsymbol{N}_D(R_3) \boldsymbol{G}(R_3, \tau_3|R_2) \boldsymbol{N}_A(R_2) \times \boldsymbol{G}(R_2, \tau_2|R_1) \boldsymbol{N}_A(R_1) \boldsymbol{p}_{eq} dR_1 dR_2 dR_3 / \langle n \rangle \quad (17)$$

This is the appropriate generalization of eq 15. Here, $\boldsymbol{N}_A(R)$ and $\boldsymbol{N}_D(R)$ are diagonal matrices with $n_{Ai}(R)$ and $n_{Di}(R)$ on the diagonal, $\langle n \rangle \propto \int \mathbf{1}^T \boldsymbol{N}(R) \boldsymbol{p}_{eq} dR$. $\boldsymbol{G}(R,t|R_0)$ is the matrix with elements $[\boldsymbol{G}(R,t|R_0)]_{ij}$, which are the probability densities of finding the molecule at (i, R) at time t given it was at (j, R_0) initially and that no photons were detected during this time. It satisfies an equation which differs from eq 14 by a term that describes translational diffusion[11]

$$\frac{\partial}{\partial t}\boldsymbol{G} = D\nabla^2 \boldsymbol{G} + \boldsymbol{K}\boldsymbol{G} - \boldsymbol{N}(R)\boldsymbol{G} \quad (18)$$

where $\boldsymbol{N}(R) = \boldsymbol{N}_A(R) + \boldsymbol{N}_D(R)$ and D is the translational diffusion coefficient of the molecule, which is assumed to be conformation-independent.

Next, we consider the conditions under which the pdf in eq 17 can be factored. Let us assume that the total count rate does not depend on the conformational coordinate

$$n_{Ai}(R) + n_{Di}(R) = n(R) \tag{19}$$

and the ratio of the acceptor count rate to the sum of donor and acceptor count rates does not depend on the translational coordinate

$$\frac{n_{Ai}(R)}{n_{Ai}(R) + n_{Di}(R)} = \epsilon_i \tag{20}$$

With these assumptions, two different quantities can be factored. First, the count rates factor as

$$\begin{aligned} n_{Ai}(R) &= n(R)\epsilon_i \\ n_{Di}(R) &= n(R)(1 - \epsilon_i) \end{aligned} \tag{21}$$

This is equivalent to $\boldsymbol{N}_A(R) = n(R)\boldsymbol{E}$ and $\boldsymbol{N}_D(R) = n(R)(\boldsymbol{I} - \boldsymbol{E})$ in matrix notation. Second, the probability of detecting no photons during a time interval also factors, as can be verified by substitution into eq 18 with $\boldsymbol{N}(R) = n(R)\boldsymbol{I}$

$$\boldsymbol{G}(R, t|R_0) = g(R, t|R_0)\mathrm{e}^{\boldsymbol{K}t} \tag{22}$$

Here, $g(R,t|R_0)$ is the propagator of translational diffusion given that no photons were detected during time t. It satisfies

$$\frac{\partial}{\partial t}g = D\nabla^2 g - n(R)g \tag{23}$$

with initial condition $g(R,0|R_0) = \delta(R - R_0)$.

Using eqs 21 and 22 in eq 17, we find that the pdf of observing the sequence of photons shown in Figure 7 can be factored as

$$f = \int n(R_3)g(R_3, \tau_3|R_2)n(R_2)g(R_2, \tau_2|R_1)n(R_1)\mathrm{d}R_1\mathrm{d}R_2\mathrm{d}R_3/\langle n\rangle \times \mathbf{1}^{\mathrm{T}}(\boldsymbol{I} - \boldsymbol{E})\mathrm{e}^{\boldsymbol{K}\tau_3}\boldsymbol{E}\mathrm{e}^{\boldsymbol{K}\tau_2}\boldsymbol{E}\boldsymbol{p}_{\mathrm{eq}} \tag{24}$$

This is the generalization of eq 16. The first factor, which is conformation-independent, is the pdf of observing the photon trajectory in Figure 7 irrespective of color. The second term, which depends only on conformational parameters, is the probability of observing the photon colors. To find the conformational parameters by optimization, one needs only to consider the probability of photon colors, that is, the second term. Thus, we can extract all information about conformational parameters from a photon trajectory without the modeling interphoton time distribution, which is difficult for diffusing molecules. The extension of the above analysis to any number of photons in a burst leads to eq 2.

Finally, we consider background noise. Suppose that the background photons are uncorrelated with the photons emitted by a molecule and have Poisson statistics with the count rates b_A for the acceptor and b_D for the donor background photons. Equation 17 for the probability of the photon trajectory in Figure 7 must be generalized to take into account that (1) a detected photon may come from the molecule or from the background and that (2) there are no photons of any kind between two successively detected photons. Therefore, $n_{Ai}(R)$ in eq 17 must be replaced by $n_{Ai}(R) + b_A$ and analogously for the donor count rate, and $\boldsymbol{G}(R,t|R_0)$ must be multiplied by $\exp(-bt)$, where $b = b_A + b_D$ is the total background count rate. As a result, eq 17 becomes

$$f = \int \mathbf{1}^{\mathrm{T}}(\boldsymbol{N}_D(R_3) + b_D\boldsymbol{I})\boldsymbol{G}(R_3, \tau_3|R_2)\mathrm{e}^{-b\tau_3}(\boldsymbol{N}_A(R_2) + b_A\boldsymbol{I}) \times \boldsymbol{G}(R_2, \tau_2|R_1)\mathrm{e}^{-b\tau_2}(\boldsymbol{N}_A(R_1) + b_A\boldsymbol{I})\boldsymbol{p}_{\mathrm{eq}}\mathrm{d}R_1\mathrm{d}R_2\mathrm{d}R_3/\langle n\rangle \tag{25}$$

Under conditions where the pdf in eq 17 factors (see eq 24), the above pdf cannot be exactly factored because the count rates do not factor. The effective efficiency in the presence of background noise depends on both translational and conformational coordinates, $\epsilon_i(R) = (n_{Ai}(R) + b_A)/(n(R) + b) = \epsilon_i + (b_A - b\epsilon_i)/(n(R) + b)$. However, if we approximate the total count rate $n(R) + b$ by its average over the laser spot, $\langle n\rangle$, then the efficiency becomes independent of the location of the molecule in the laser spot

$$\epsilon_i(R) \approx \epsilon_i^{\mathrm{fit}} \equiv \epsilon_i(1 - (b_A + b_D)/\langle n\rangle) + b_A/\langle n\rangle \tag{26}$$

We can now factor eq 25, analogously to eq 24, by using an apparent efficiency $\epsilon_i^{\mathrm{fit}}$, which is related to the efficiency corrected for background noise by eq 26.

The above correction procedure is exact for Poissonian background photons and immobilized molecules. In the case of diffusing molecules, it is based on the approximation that the total count rate can be replaced by its average over the laser spot. This is valid when the fluctuations of the total count rate in the laser spot are small or the noise is small, $(b_A + b_D)/\langle n\rangle \ll 1$.

V. Concluding Remarks

In this paper, we have presented an approach to extract information about interdye distances and conformational dynamics from the observed sequence of photons with specified colors and photon arrival times. The conformation-dependent energy transfer efficiencies and the rates of interconversion are obtained by maximizing the appropriate likelihood function. In contrast to using FRET efficiency histograms, this approach does not involve binning, and therefore, all of the information contained in the observed photon trajectory is used. The procedure is applicable to data collected for both diffusing and immobilized molecules. Both shot noise and background noise can be accounted for.

When the sum of acceptor and donor photons does not depend on conformation, one can analyze only the sequence of photon colors. This is particularly advantageous for diffusing molecules because the difficult problem of modeling the interphoton times is bypassed. Another advantage of this method is that it is insensitive to how bursts of photons are defined, as long as the burst selection is unbiased.

Once the apparent efficiencies of the states are extracted, they can be related to more microscopic conformational parameters such as interdye distances. It is at this stage that fast photophysical and conformational processes as well as experimental complications such as direct excitation of the acceptor are

handled. All of these effects simply alter the dependence of the apparent FRET efficiency on the interdye distance.

The likelihood function that is maximized depends on the underlying kinetic scheme which describes the number of conformational states, their connectivity, and the rates of interconversion. By including different states with the same efficiency, we can describe conformations that have multiexponential residence (waiting) time distributions. Finally, we wish to point out that our formalism can also handle models where conformational space is continuous (e.g., diffusion on a potential of mean force) by discretizing space and constructing the rate matrix from the finite difference approximation of the appropriate operator.

Acknowledgment. We thank A. M. Berezhkovskii, H. S. Chung, W. A. Eaton, D. Nettels, and B. Schuler for helpful comments and the NIH Fellows Editorial Board for editorial assistance. This work was supported by the Intramural Research Program of the National Institutes of Health, NIDDK.

References and Notes

(1) Michalet, X.; Weiss, S.; Jäger, M. *Chem. Rev.* **2006**, *106* (5), 1785–1813.
(2) Moerner, W. E. *Proc. Natl. Acad. Sci. U.S.A.* **2007**, *104* (31), 12596–12602.
(3) Schuler, B.; Eaton, W. *Curr. Opin. Struct. Biol.* **2008**, *18*, 16–26.
(4) Schuler, B. *ChemPhysChem* **2005**, *6*, 1206–1220.
(5) Antonik, M.; Felekyan, S.; Gaiduk, A.; Seidel, C. A. M. *J. Phys. Chem. B* **2006**, *110* (13), 6970–6978.
(6) Nir, E.; Michalet, X.; Hamadani, K. M.; Laurence, T. A.; Neuhauser, D.; Kovchegov, Y.; Weiss, S. *J. Phys. Chem. B* **2006**, *110* (44), 22103–22124.
(7) Watkins, L.; Chang, H.; Yang, H. *J. Phys. Chem. A* **2006**, *110* (15), 5191–5203.
(8) Merchant, K. A.; Best, R. B.; Louis, J. M.; Gopich, I. V.; Eaton, W. A. *Proc. Natl. Acad. Sci. U.S.A.* **2007**, *104* (5), 1528–1533.
(9) Kalinin, S.; Felekyan, S.; Valeri, A.; Seidel, C. *J. Phys. Chem. B* **2008**, *112* (28), 8361–8374.
(10) Gopich, I. V.; Szabo, A. *J. Phys. Chem. B* **2003**, *107* (21), 5058–5063.
(11) Gopich, I. V.; Szabo, A. *J. Phys. Chem. B* **2007**, *111* (44), 12925–12932.
(12) Gopich, I.; Szabo, A. *J. Chem. Phys.* **2005**, *122* (1), 147071−18.
(13) Horn, R.; Lange, K. *Biophys. J.* **1983**, *43* (2), 207–223.
(14) Colquhoun, D.; Hawkes, A.; Srodzinski, K. *Philos. Trans. R. Soc. London, Ser. A* **1996**, *354* (1718), 2555–2590.
(15) Qin, F.; Auerbach, A.; Sachs, F. *Biophys. J.* **2000**, *79* (4), 1915–1927.
(16) Milescu, L.; Yildiz, A.; Selvin, P.; Sachs, F. *Biophys. J.* **2006**, *91* (4), 1156–1168.
(17) Witkoskie, J. B.; Cao, J. *J. Phys. Chem. B* **2008**, *112* (19), 5988–5996.
(18) Andrec, M.; Levy, R. M.; Talaga, D. S. *J. Phys. Chem. A* **2003**, *107* (38), 7454–7464.
(19) Schröder, G. F.; Grubmüller, H. *J. Chem. Phys.* **2003**, *119* (18), 9920–9924.
(20) Watkins, L. P.; Yang, H. *J. Phys. Chem. B* **2005**, *109* (1), 617–628.
(21) Kou, S. C.; Xie, X. S.; Liu, J. S. *J. R. Stat. Soc., Ser. C* **2005**, *54* (3), 469.
(22) McKinney, S.; Joo, C.; Ha, T. *Biophys. J.* **2006**, *91* (5), 1941–1951.
(23) Munro, J.; Vaiana, A.; Sanbonmatsu, K.; Blanchard, S. *Biopolymers* **2008**, *89* (7), 565–577.
(24) Gell, C.; Brockwell, D.; Smith, D. A. *Handbook of single molecule fluorescence spectroscopy*; Oxford University Press: New York, 2006.
(25) Best, R. B.; Merchant, K. A.; Gopich, I. V.; Schuler, B.; Bax, A.; Eaton, W. A. *Proc. Natl. Acad. Sci. U.S.A.* **2007**, *104* (48), 18964–18969.
(26) Gopich, I. V. *J. Phys. Chem. B* **2008**, *112* (19), 6214–6220.
(27) Gillespie, D. *Markov processes: an introduction for physical scientists*; Academic Press: New York, 1992.
(28) Schwarz, G. *Ann. Stat.* **1978**, *6*, 461–464.
(29) MacKay, D. *Information theory, inference and learning algorithms*; Cambridge University Press: New York, 2003.
(30) Sivia, D. S. *Data analysis: A Bayesian tutorial*; Oxford University Press: New York, 2006.
(31) Milescu, L.; Akk, G.; Sachs, F. *Biophys. J.* **2005**, *88* (4), 2494–2515.
(32) Chung, H. S.; Louis, J. M.; Eaton, W. A. *Proc. Natl. Acad. Sci. U.S.A.* **2009**, *106* (29) 11837–11844.
(33) Gopich, I. V.; Szabo, A. *J. Chem. Phys.* **2006**, *124* (15), 154712/1–154712/21.
(34) Gopich, I. V.; Szabo, A. *In Theory and Evaluation of Single-Molecule Signals*; Barkai, E., Brown, F. L. H., Orrit, M., Yang, H., Eds.; World Scientific Publishing Co. Inc.: River Edge, NJ, 2008; pp 181−244.
(35) Witkoskie, J. B.; Cao, J. *J. Chem. Phys.* **2004**, *121* (13), 6373–6379.
(36) In the literature, the efficiency is often defined as $E = n_A/(n_A + \gamma n_D)$, in which case the relation between E and r is simply $E = (1 + (r/R_0)^6)^{-1}$. Our definition is more natural when photon count statistics are analyzed. Both efficiencies can be converted to the same interdye distance if one uses the appropriate relationships.

JP903671P